

## Structure and energetics of $H_{15}^+$ hydrogen clusters

B. Farizon and M. Farizon

*Institut de Physique Nucléaire de Lyon (CNRS-IN2P3), 43 boulevard du 11 novembre 1918, F-69622 Villeurbanne Cedex, France*

H. Razafinjanahary

*Laboratoire de Chimie Physique Théorique, bâtiment 210, Université Claude Bernard, 43 boulevard du 11 novembre 1918, F-69622 Villeurbanne Cedex, France*

H. Chermette

*Laboratoire Chimie Physique Théorique, bâtiment 210, Université Claude Bernard, 43 boulevard du 11 novembre 1918, F-69622 Villeurbanne Cedex, France*  
*and Institut de Recherches sur la Catalyse, UPR CNRS 5401, 2 avenue Albert Einstein, F-69626 Villeurbanne Cedex, France*

(Received 14 December 1998)

Low-lying stationary points on the  $H_{15}^+$  potential energy hypersurface have been determined through Hartree-Fock (HF) calculations and density functional theory (DFT) with the recently proposed functional especially designed for hydrogen systems [B3(H)]. Calculations have been carried out for three conformers of  $H_{15}^+$  ( $C3v$ ,  $Cs$ , and  $D3h$  symmetries) leading to fully optimized structures and energies. Only the  $C3v$  and  $Cs$  structures are true minima. The total energy of the  $Cs$  structure lies  $10^{-4}$  Hartrees lower than the  $C3v$  one. Vibrational frequencies and infrared intensities for both stationary points have been predicted within HF and DFT B3(H) methods. [S0163-1829(99)12029-0]

### I. INTRODUCTION

Ionic clusters such as  $H_3^+(H_2)_n$  are important species in the stratosphere,<sup>1</sup> where molecules readily nucleate about ions as a result of the long-range attractive forces dominating ion-molecule interactions. Such weakly bound molecular cluster ions have thus attracted much attention. Clampitt and Gowland<sup>2</sup> observed  $H_5^+$  up to  $H_{47}^+$  odd-numbered clusters by sweeping a low-energy electron beam over a condensed  $H_2$  surface. Their initial mass distribution showed  $H_{15}^+$  to be one of the most abundant ions. For this  $H_{15}^+$  ion, they proposed an octahedral structure of the general form  $H_3^+(H_2)_n$ . Van Lumig and Reuss<sup>3</sup> measured the dissociation cross section of hydrogen clusters with He target in the projectile kinetic energy range. They suggested the existence of particularly stable  $H_9^+$ ,  $H_{15}^+$ ,  $H_{19}^+$ , and  $H_{23}^+$ . The gas-phase clustering reaction  $H_3^+(H_2)_{n-1} + H_2 \rightarrow H_3^+(H_2)_n$  has been studied by several investigators.<sup>4</sup> Hiraoka and Mori<sup>4</sup> have studied the thermochemical properties and stabilities of  $H_3^+(H_2)_n$  clusters and suggested a successive shell formation for the clusters  $H_3^+(H_2)_n$  with  $n=3, 6, 8,$  and  $10$ . Bae and co-workers<sup>5</sup> have also observed shell formation for the clusters  $H_3^+(H_2)_n$  sequentially grown on seed positive ions generated by electron impact ionization in a pulsed supersonic jet. They suggested a pentagonal bipyramid structure for the  $H_{15}^+$  ionic cluster. The  $H_{15}^+$  system is of special interest since it has often been experimentally observed to possess a relatively high stability.

Theoretical descriptions of the smallest clusters of the  $H_{2n+1}^+$  family have been given at various levels of theory. They belong either to the *ab initio* [Hartree-Fock (HF) and post-HF] models, or the density functional theory (DFT) ap-

proach. This last case includes both Kohn-Sham (KS) (Ref. 6) and Car-Parrinello (CP) calculations.<sup>7</sup> The structure of the  $H_3^+(H_2)_n$  clusters are generally described as  $H_2$  units surrounding an  $H_3^+$  core. These clusters are very weakly bounded and require fairly large basis sets for covering results. To our knowledge, only one *ab initio* calculation has been performed yet beyond  $H_{13}^+$  by Diekmann *et al.*<sup>8</sup>

In a recent paper,<sup>9</sup> Stich *et al.* carried out a quantum simulation bearing on  $H_3^+$ ,  $H_5^+$ ,  $H_7^+$ ,  $H_9^+$ , and  $H_{27}^+$ . Their Car-Parrinello calculations showed that the  $H_2$  molecules constituting the solvation shells around the tightly localized  $H_3^+$  core are weakly bonded. This feature affects mostly the rotations of the solvating  $H_2$  in what they called a “quantum plasticity” since classical simulations would lead to more rigid clusters.<sup>9,10</sup> These conclusions are in good agreement with the flat potential energy surface (PES) we obtain through the geometry optimizations processes performed in the present work and previous calculations.<sup>11-13</sup> However Stich *et al.*<sup>9</sup> used for their dynamics forces calculations within Kohn-Sham DFT formalism using the PW91 (Ref. 15) exchange-correlation functional. Although they claimed that the structures they obtained agree within 5% on average with our reference structures (and even within less than 3% for the largest clusters, probably  $H_{11}^+ - H_{13}^+$ ), this hides large deviations for the smallest clusters, namely,  $H_5^+$  and  $H_7^+$ .<sup>10</sup> Indeed, we have shown<sup>11</sup> that any popular DFT functional (GGAs, B3LYP, . . .) of the time being are unable to describe properly  $H_5^+$ .

The aim of this paper is to describe the properties and structure of the  $H_{15}^+$  ion which has been claimed in the past to be especially stable. For this purpose because the HF method is known to be insufficiently accurate to describe properly weakly bonded or highly correlated systems, we have recently performed calculations using a DFT functional

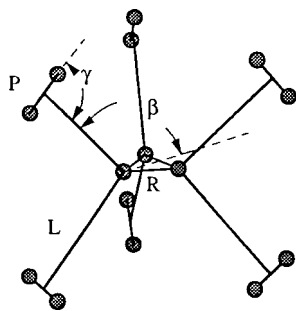


FIG. 1.  $H_{15}^+$  optimized structure in  $D3h$  symmetry.

especially designed for such systems [named  $B3(H)$ ].<sup>11</sup> We report here on theoretical prediction of the structures and energies of three conformers of  $H_{15}^+$  with  $C_s$ ,  $C3v$ , and  $D3h$  symmetries. The corresponding vibrational frequencies (calculated within the harmonic approximation) and infrared intensities are also given. Some concluding remarks will be given bearing on the adequacy of both HF and DFT models [with the  $B3(H)$  functional] for the description of hydrogenic clusters.

## II. THEORETICAL APPROACH

In previous theoretical studies,<sup>12,13</sup> *ab initio* self-consistent-field Hartree-Fock (SCF) and configuration interaction (CI) calculations have been carried out for  $H_3^+(H_2)_n$  ( $n=1-5$ ) clusters using a triple-zeta plus polarization basis set. Especially, we found that the structures of  $H_{11}^+$  and  $H_{13}^+$  clusters<sup>13</sup> can be viewed as resulting of the addition of  $H_2$  molecules to a weakly deformed  $H_9^+$  core. Because the computational effort increases as  $n^6$  for CISD calculations (which are not size consistent),  $n^7$  for CCSD(T) ( $n$  being the size of the basis set which is proportional to the number of atoms), some of us developed recently a density functional which allows one to tackle the hydrogen clusters problem within DFT.<sup>11</sup> In DFT the computational effort scales formally as  $n^3$  for LDA or GGA approximations and  $n^4$  for hybrid functionals which contain some HF exchange. Indeed, with efficient codes, the computational effort can be reduced up to  $n^{2.7}$ , thanks to cutoffs for integral computations.

This functional named  $B3(H)$  has been proved to lead to geometries and energies of  $H_{2n+3}^+$  clusters which are close to those obtain through CCSD(T) calculations, which for these kind of species are not very different to CISD ones. The parametrization of the  $B3(H)$  functional was fitted on  $H_5^+$  structure, and found adequate for all clusters sizes from  $H_3^+$  to  $H_{13}^+$ .<sup>11</sup>

In the present work, we extend our work of characterization of  $H_{2n+3}^+$  species to the  $H_{15}^+$  ion. The computations were performed with the Gaussian 94 package.<sup>16</sup> The  $H_{15}^+$  cluster structure has been computed at three levels of theory, HF, CISD, and DFT/ $B3(H)$ . In a previous paper,<sup>11</sup> we have studied the accuracy of the basis sets and found that the 6-311G\*\* (unfortunately misprinted ++ in Ref. 11) was satisfactory for this kind of systems. This basis set has been retained as well in Farizon *et al.*, post Hartree-Fock work.<sup>12</sup> In order to test the quality of this basis set for bigger systems, which could be poorly described in the external shell

TABLE I. Typical parameters of the optimized geometries of  $H_{15}^+$  with  $D3h$  symmetry at HF,  $B3(H)$ /DFT levels of theory. Parameters are defined in Fig. 1.

Method	$R$ (pm)	$H$ (pm)	$\beta$ (deg.)	$P$ (pm)	$\gamma$ (deg.)	energy (a.u.)
HF	86.7	222.3	134.9	73.8	90.8	-8.1088
$B3(H)$	87.4	200.4	136.1	74.0	90.0	-8.4117

of the  $H_2$  units, we have also performed the calculations with the 6-311G\*\*. Hence we verified that neither the frequency patterns (shifted at most by 4  $\text{cm}^{-1}$ ) nor the energetics were significantly altered by the change of basis set. This is explained easily by the fact that the  $H_{2n+1}^+$  clusters are charged species. In addition to HF and  $B3(H)$  calculations, a post-Hartree-Fock calculation of a given structure, namely, the  $C_s$  one, has also been performed within the CISD method. Since this method is not size consistent, size consistency corrections (SCC's) have been estimated according to Davidson's scheme, as in Ref. 13. Full geometry optimizations have been done, the optimization being stopped when the magnitude of the gradient becomes below  $10^{-5}$  a.u. Vibration frequencies have been evaluated within harmonic approximation from the second derivative analysis.

## III. STRUCTURES

### A. $D3h$ structure

Figure 1 shows the fully optimized geometry of  $H_{15}^+$  with  $D3h$  symmetry, predicted at the HF level of theory. The optimized structure and the predicted energy are compiled in Table I. In this structure, six  $H_2$  are arranged symmetrically around the  $H_3^+$  core. Two pairs of the three  $H_2$  molecules are lying above and below of the  $H_3^+$  plane. The distance  $R$  (86.71 pm) is smaller than those found in the

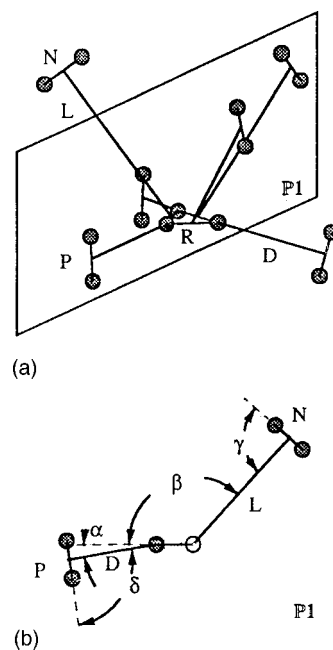


FIG. 2.  $H_{15}^+$  optimized structure in  $C3v$  symmetry.

TABLE II. Typical parameters of the optimized geometries of  $H_{15}^+$  with  $C3v$  symmetry at HF, B3(H)/DFT levels of theory. Parameters are defined in Fig. 2.

Method	$R$ (pm)	$D$ (pm)	$\alpha$ (deg.)	$L$ (pm)	$\beta$ (deg.)	$P$ (pm)	$N$ (pm)	$\gamma$ (deg.)
HF	87.5	179.1	11.5	287.7	132.7	74.1	73.7	88.7
B3(H)	88.6	165.8	8.4	283.5	132.3	74.5	73.8	87.1

other structures by approximately 1 pm. The distance  $H$  is found to be smaller than the distances  $L(H_9^+-H_2)$  but greater than the corresponding distance  $D(H_3^+-H_2)$  in the  $Cs$  and  $C3v$  structures. However, at the HF level, the harmonic vibration analysis exhibits one imaginary frequency, so that the structure could be thought as being a transition state between two  $C3v$  structures. Within DFT, the B3(H) structure is qualitatively the same with slightly longer bonds in the  $H_2$  units or the  $H_3^+$  core, and a shorter (10%) distance between the  $H_2$  and the  $H_3^+$  core. The vibrational analysis leads to even more imaginary frequencies, since eight imaginary frequencies are found.

The total energy, significantly higher than the  $C3v$  and  $Cs$  ones, indicates also that this structure is rather a transition state.

### B. $C3v$ structure

On the basis of our previous work on  $H_{11}^+$  and  $H_{13}^+$ , the  $C3v$  structure is obtained by addition of three  $H_2$  molecules to a  $H_9^+$  core (where the  $H_2$  subunits lie nearly perpendicular to the  $H_3^+$  plane). Figure 2 shows the fully optimized geometry for  $H_{15}^+$  with  $C3v$  symmetry assignment, predicted at HF level of theory. The optimized parameters structure and the predicted energy are reported in Tables II and IV. Starting from  $H_9^+$ , each further  $H_2$  molecule is located in a mediator plane perpendicular to the  $H_3^+$  and going through one apex of the  $H_3^+$  triangle [see plan P1, inset in Fig. 2(a)]. A deformation of the  $H_9^+$  core is observed (angle  $\alpha=11.5^\circ$ ) stronger than for the  $Cs$  structure of  $H_{15}^+$  (*vide supra*). The distance  $L$  between each added  $H_2$  subunits and

the deformed  $H_9^+$  core, about 287 pm, is 1 pm smaller than the corresponding distance in  $H_{13}^+$ , 1 pm larger than the corresponding distance in  $H_{11}^+$ . The distances between the outer  $H_2$  subunits are on the order 382 pm. This structure is a true minimum in the potential energy surface of  $H_{15}^+$  at this level of theory.

Within the DFT approach, the structure obtained does not differ significantly with the one optimized at HF level described above and is also a true minimum. The main differences lie in shorter  $H_3^+-H_2$  distances, in particular  $D$  which concerns the first  $H_2$  shell i.e., the  $H_9^+$  core. Concomitantly, the  $H_3^+$  nucleus is slightly relaxed.

### C. $Cs$ structure

Figure 3(a) shows the fully optimized geometry of  $H_{15}^+$  with  $Cs$  symmetry, predicted at the three both levels of theory HF, CISD, and DFT/B3(H). The optimized structures and the predicted energies are gathered in Tables III and IV. This structure is also a true minimum. The  $Cs$  structure is built by addition of three  $H_2$  molecules to a  $H_9^+$  core as the previous structure, but placing two  $H_2$  subunits on one side of the  $H_9^+$  core and the last  $H_2$  on the opposite side [see Fig. 3(a)]. These outer  $H_2$  are found to be off centered with respect to the center of the  $H_3^+$  core. A deformation of the  $H_9^+$  core is observed:  $H_2$  subunits link the  $H_3^+$  plane with an angle  $\alpha_2=9.5^\circ$  for both of them and  $\alpha_1=6.7^\circ$  for the third one [see Fig. 3(b)]. Moreover, the distances  $D1$  and  $D2$  are found to differ by 2.36 pm and the central  $H_3^+$  core is not anymore equilateral. The same trend is kept for the CISD and the B3(H) calculations.

TABLE III. Typical parameters of the optimized geometries of  $H_{15}^+$  with  $Cs$  symmetry at HF, CISD, B3(H)/DFT levels of theory. Parameters are defined on Fig. 3.

Method	$R1$ (pm)	$R2$ (pm)	$D1$ (pm)	$\alpha1$ (deg.)	$D2a$ (pm)	$D2b$ (pm)	$\alpha2$ (deg.)	$L1$ (pm)
HF	87.5	87.6	179.7	6.7	99.1	190.8	9.5	297.4
CISD	88.6	88.7	168.4	6.8	91.3	183.0	4.5	282.3
B3(H)	88.6	88.9	167.2	2.4	89.3	182.4	4.1	277.7

	$\beta1$ (deg.)	$L2a$ (pm)	$L2b$ (pm)	$\beta2$ (deg.)	$P1$ (pm)	$\delta1$ (deg.)	$P2$ (pm)	$\epsilon$ (deg.)
HF	84.3	258.4	184.6	60.4	74.2	90.2	74.2	85.4
CISD	86.9	248.7	174.7	59.8	74.8	90.3	74.8	83.1
B3(H)	95.3	242.8	172.0	60.2	74.4	90.4	74.5	81.4

	$\delta2$ (deg.)	$N1$ (pm)	$\gamma1$ (deg.)	$N2$ (pm)	$\eta$ (deg.)	$\gamma2$ (deg.)
HF	97.1	73.7	108.1	73.7	136.8	74.5
CISD	101.0	74.1	103.9	74.1	132.9	65.0
B3(H)	95.9	73.8	105.2	73.8	130.5	70.5

TABLE IV. Total energies and dissociation energies (according to  $H_{15}^+ \rightarrow H_2 + H_{13}^+$ ) of the optimized geometries of  $H_{15}^+$  with  $C_s$  and  $C3v$  symmetries at HF,  $B3(H)$ /DFT levels of theory. The corresponding zero-point energies (ZPE's) are also given.

Method	Total energies (a.u.)	Dissociation energies ( $D_e$ ) (kJ mol <sup>-1</sup> )	ZPE (a.u.)
<i>C3v</i> symmetry			
HF	-8.1139	1.95	0.1005
$B3(H)$	-8.4185	2.86	0.1012
<i>Cs</i> symmetry			
HF	-8.1140	2.22	0.1004
CISD <sup>a</sup>	-8.3531 <sup>b</sup>	3.14	
$B3(H)$	-8.4186	3.12	0.1014

<sup>a</sup>CISD energy calculated at HF geometry.

<sup>b</sup>Size-consistency correction estimated to -0.02188 a.u.

It is remarkable that all the calculations predict that this structure is more stable than the  $C3v$  one, but the energy difference between the two stable structures amounts only  $10^{-4}$  Hartree (0.03 eV). Typical distances representative of the  $H_3^+ - H_2$  interaction ( $D$ ), the  $H_9^+ - H_2$  interaction ( $L$ ), the  $H_3^+$  core ( $R$ ), and the  $H_2$  subunits ( $P$  and  $N$ ), have been reported in Fig. 4 for the whole series of clusters  $H_{2n+3}^+$ ;  $n=1, 6$  as obtained in HF and  $B3(H)$  calculations. When two distances, for example,  $P1$  and  $P2$  are representative of a distance  $P$ , both of them are reported on Fig. 4. We can see that the typical distances of  $C_s - H_{15}^+$  follow the same general trend already pointed out with  $H_{11}^+$  and  $H_{13}^+$ .  $D$  increases with the mass number and reach a nearly constant value ( $\sim 177$  pm) for  $n$  greater than 3. On the other hand, comparing the distances  $R$  between the protons in the  $H_3^+$  core one can notice that this core is less deformed in the  $H_{15}^+$  cluster than in the  $H_{13}^+$  cluster. The distances  $P$  in the  $H_2$  subunits within the  $H_9^+$  core decrease with  $n$  up to a nearly constant value (74.2 pm for  $H_{15}^+$  at HF level). The distances  $N$  (73.8 pm) in all other  $H_2$  subunits in  $H_{15}^+$ , i.e., the most external are even smaller than the distances  $P$  and closer to the 73.6 pm value of free  $H_2$ . In order to compare efficiently the distance representing the interaction  $H_9^+ \cdots H_2$  in  $H_{11}^+$ ,  $H_{13}^+$ , and  $H_{15}^+$ , we have reported on Fig. 4 the distance  $C$  corresponding to the distance between the outer  $H_2$  subunits and the center of  $H_3^+$ . The values obtained for  $C$  amounts in HF calculations 290.8, 293.4 and 303.4, 308.3 pm for  $H_{11}^+$ ,  $H_{13}^+$ , and  $H_{15}^+$ , respectively. In the  $B3(H)$  calculation the values are 279.7, 281.3 and 287.9, 288.2 pm, respectively. The value of distance  $C$  in  $H_{15}^+$  is 10 pm greater than the value obtained for the other clusters at HF level, the difference is slightly reduced with  $B3(H)$ . We notice that the  $C_s$  structure of  $H_{15}^+$  includes a pair of  $H_2$  molecules on one side of the  $H_9^+$  core. The distance between the  $H_2$  molecule has been estimated about 349 pm in HF and 341 pm in  $B3(H)$  calculation in this pair, which is not far from the value (344 pm) of the intramolecular distance of the solid hydrogen.<sup>14</sup>

#### IV. ENERGETICS

The stability of the clusters can be investigated through the dissociation energies of these clusters according to the

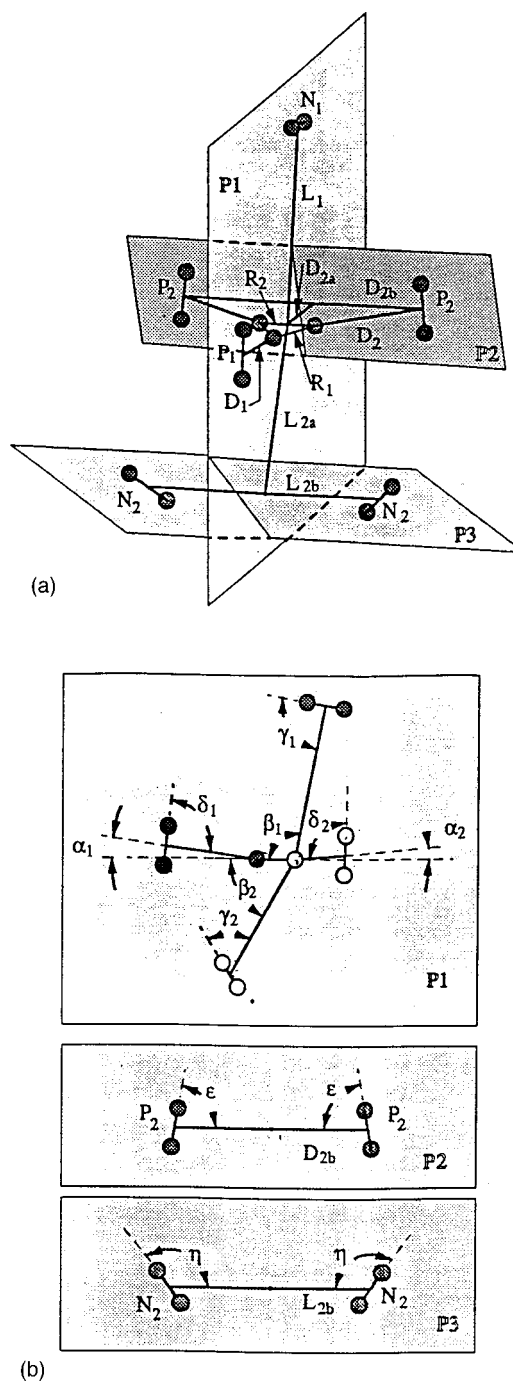
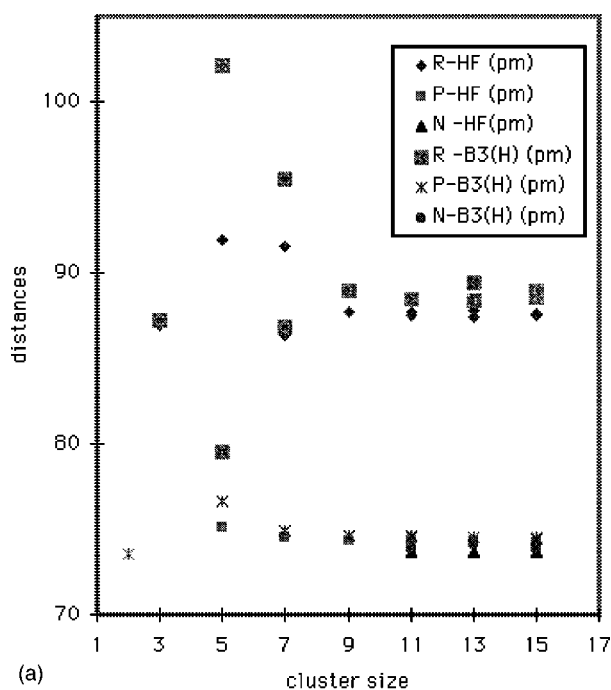
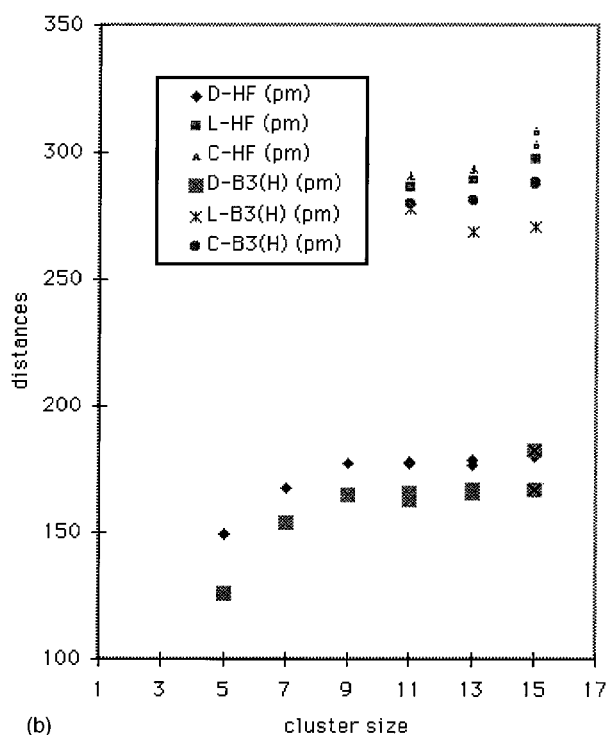


FIG. 3.  $H_{15}^+$  optimized structure in  $C_s$  symmetry.

reaction  $H_3^+(H_2)_{n-1} + H_2 \rightarrow H_3^+(H_2)_n$ . As in previous works,<sup>11-13</sup> the dissociation energies  $D_e$  for the abstraction of molecular hydrogen from  $H_{15}^+$  are deduced from the calculation at HF and  $B3(H)$  levels of theory for the three conformers and sake of comparison at CISD for the  $C_s$  conformer. The energies required to remove molecular hydrogen from  $C_s - H_{15}^+$ ,  $C3v - H_{15}^+$ , and  $D3h - H_{15}^+$  are 2.22, 1.95, and  $-1.16$  kJ, respectively, for HF calculations and 3.12, 2.86, and  $-14.9$  kJ for  $B3(H)$  calculations, to be compared to the experimental value ( $7.27 \pm 0.42$ ) kJ. In Fig. 5 it has been reported together to previous values<sup>11-13</sup> the dissociation energies of  $H_3^+(H_2)_n$   $n=1-6$  as calculated within HF



(a)



(b)

FIG. 4. Typical bond lengths of the optimized geometries of  $H_3^+(H_2)_n$ ,  $n=1-6$  at HF and  $B3(H)/DFT$  levels of theory.

and  $B3(H)$ . The predicted dissociation energies  $De$  of  $H_{15}^+$  is found to follow the experimental trend established by Hiraoka and Mori,<sup>4</sup> as for the other cluster sizes. The gap between the stabilities of the  $H_5^+-H_7^+-H_9^+$  group and the  $H_{11}^+-H_{13}^+$  group is kept similar for  $H_{15}^+$ . This indicates that  $H_{15}^+$  would not exhibit an enhanced stability (magic number) as proposed in Ref. 3, but not seen in Ref. 17. These energies are definitely lower than those obtained by Stich *et al.* in their simulations,<sup>10</sup> but the reason lies in the gener-

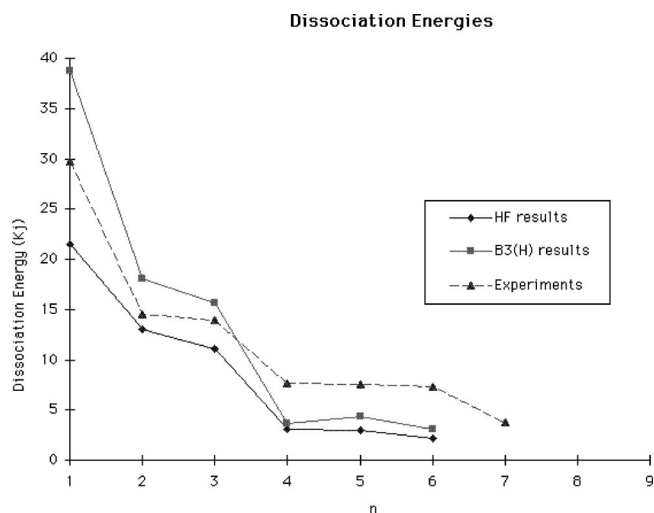


FIG. 5. Theoretical [HF and  $B3(H)$  level of theory] and experimental (Ref. 4) values of dissociation energies of  $H_3^+(H_2)_n$ ,  $n=1-6$ .

alized gradient approximation they used (namely PW91) which is known to be more bonding for van der Waals systems.<sup>18,19</sup>

At the CISD level of theory, a similar poor agreement is obtained for the  $De(Cs-H_{15}^+)$  value, 3.14 kJ, similar to that for  $H_{11}^+$  and  $H_{13}^+$ . As previously mentioned, this is traditionally related to the weakness of the size consistency corrections which are not sufficient. In this kind of system, the size consistency error is rather weak because of the large distance between the  $H_2$  units.

## V. VIBRATIONAL FREQUENCIES

Harmonic vibrational frequencies were predicted for the  $Cs$  and  $C3v$  conformers of  $H_{15}^+$  clusters from HF and  $B3(H)$  calculations. The results are shown in Tables V and VI. In the  $Cs-H_{15}^+$  case, six frequencies among the 39 distinct ones correspond to those arising from the stretching linking the first three  $H_2$  subunits to the  $H_3^+$  core [4503, 4497, 4496, 3427, 2685, 2664  $cm^{-1}$  with HF and 4436, 4426, 4424, 3269, 2477, 2465  $cm^{-1}$  at  $B3(H)$  level]. Our results exhibit nearly the same theoretical vibrational frequencies as in  $H_9^+$  isolated cluster (4492, 4487 degenerate, 3406, 2656 degenerate  $cm^{-1}$  estimated at HF level of theory<sup>12</sup>) and [4424, 4416 degenerate, 3243, 2459, 2447 with  $B3(H)$  calculation<sup>11</sup>], due to the weak deformation of the  $H_3^+$  core by approaching three  $H_2$  ligands. One of highest mode and the three highest frequencies at 4575, 4574, and 4573  $cm^{-1}$  [4527, 4526, and 4525  $cm^{-1}$  with  $B3(H)$ ] correspond to the three external  $H_2$  vibrations result from the supplementary modes of  $H_{15}^+$  brought by addition of one  $H_2$  to  $H_{13}^+$ . Due to the weak  $H_9^+-H_2$  interaction, these vibrational frequencies are smaller than the harmonic frequency predicted for the isolated molecule (4594  $cm^{-1}$  (HF) and 4553  $cm^{-1}$  [ $B3(H)$ ]). These frequencies are also present in  $H_{11}^+$  and  $H_{13}^+$  (4573  $cm^{-1}$ ) spectra. Similar features are obtained in the  $C3v-H_{15}^+$  case. Taking into account the overestimation of the frequencies inherent to HF method and

TABLE V. Harmonic vibrational frequencies ( $\text{cm}^{-1}$ ) and infrared intensities (in  $\text{km/mol}$ ) with  $C_s$  symmetry at the HF and  $B3(\text{H})/\text{DFT}$  levels of theory. No scaling factor has been applied to the frequencies. The increasing order of frequencies has been slightly altered in order to put identical modes in regard, when possible.

$B3(\text{H})$			HF		
Frequencies	Intensities	Mode	Frequencies	Intensities	Mode
25	3.9	$A''$	8.2	5.1	$A''$
43	18.2	$A'$	36	18.1	$A'$
88	12.2	$A''$	62	8.3	$A''$
90	7.7	$A'$	76	7.3	$A'$
107	0.4	$A''$	78	1.4	$A''$
120	15.2	$A''$	88	12.7	$A''$
140	3.8		100	15.9	$A''$
141	9.1	$A'$	109	12.0	$A'$
143	13.3		118	15.6	$A'$
152	2.7	$A'$	120	2.9	$A'$
162	3.5	$A'$	125	0.1	$A'$
163	9.5		129	17.3	$A''$
177	1.2	$A''$	137	0.4	$A''$
185	1.7	$A''$	151	0.4	$A''$
197	73.8	$A'$	155	71.6	$A'$
201	11.2	$A'$	160	0.4	$A'$
206	0.4	$A'$	160	0	$A'$
232	19.9	$A'$	193	58.2	$A'$
298	20.1	$A'$	268	35.6	$A'$
308	16.8	$A''$	293	26.9	$A''$
323	13.1	$A'$	303	22.8	$A'$
432	448	$A'$	347	265	$A'$
459	555	$A''$	374	420	$A''$
477	92.8	$A'$	371	151	$A'$
640	4.4	$A'$	597	3.3	$A'$
649	0.3	$A''$	599	1.5	$A''$
728	9.8	$A'$	691	9.9	$A'$
822	1.3	$A''$	700	1.3	$A''$
858	0.5	$A'$	764	0.4	$A'$
881	0.4	$A''$	771	0.2	$A''$
2465	931	$A''$	2664	746	$A''$
2477	859	$A'$	2685	701	$A'$
3269	1.9	$A'$	3427	1.8	$A'$
4424	103	$A''$	4496	85.4	$A''$
4426	84.2	$A'$	4497	78.3	$A'$
4436	26.3	$A'$	4503	16.3	$A'$
4525	6.8	$A''$	4573	4.0	$A''$
4526	18.1	$A'$	4574	7.0	$A'$
4527	1.9	$A'$	4575	2.5	$A'$

$B3(\text{H})$  method (because its inclusion of some pure exchange) is usually referred to an anharmonicity correction, although it originates to the stiffness of the HF potential well. Using a scaling factor of 0.89 for HF calculations and 0.91 for  $B3(\text{H})$  frequencies as explained in Ref. 11, one gets values which are more suitable to be compared to experiment, but the trends discussed here are not altered.

Turning to the symmetric stretching frequency of  $\text{H}_3^+$ , we found 3427 (3269) and 3433 (3278)  $\text{cm}^{-1}$  for  $C_s$  and

TABLE VI. Harmonic vibrational frequencies ( $\text{cm}^{-1}$ ) and infrared intensities (in  $\text{km/mol}$ ) with  $C3v$  symmetry at the HF and  $B3(\text{H})/\text{DFT}$  levels of theory. No scaling factor has been applied to the frequencies. The increasing order of frequencies has been slightly altered in order to put identical modes in regard, when possible.

$B3(\text{H})$			HF		
Frequencies	Intensities	Mode	Frequencies	Intensities	Mode
50	0	$A_2$	42	0	$A_2$
55	0.3	$E$	51	0.6	$E$
55	0.3	$E$	51	0.6	$E$
84	12.8	$A_1$	81	15.8	$A_1$
116	0.7	$E$	94	10.0	$E$
116	0.7	$E$	94	10.0	$E$
134	11.2	$E$	109	8.5	$E$
134	11.2	$E$	109	8.5	$E$
152	0	$A_2$	115	0	$A_2$
159	11.9	$E$	132	11.5	$E$
159	11.9	$E$	132	11.5	$E$
170	102	$A_1$	132	105	$A_1$
166	0	$A_2$	148	0	$A_2$
176	0.7	$E$	148	2.2	$E$
176	0.7	$E$	148	2.2	$E$
198	1.0	$E$	159	0.1	$E$
198	1.0	$E$	159	0.1	$E$
221	23.2	$A_1$	182	41.4	$A_1$
313	29.1	$E$	296	68.3	$E$
313	29.1	$E$	296	68.3	$E$
332	1.6	$A_1$	311	1.8	$A_1$
430	536	$E$	345	389	$E$
430	536	$E$	345	389	$E$
465	4.0	$A_1$	358	4.1	$A_1$
644	5.9	$E$	601	6.4	$E$
644	5.9	$E$	601	6.4	$E$
717	9.4	$A_1$	683	10.3	$A_1$
802	0	$A_2$	679	0	$A_2$
865	3.1	$E$	763	1.1	$E$
865	3.1	$E$	763	1.1	$E$
2481	868	$E$	2682	707	$E$
2481	868	$E$	2682	707	$E$
3278	10.8	$A_1$	3433	6.1	$A_1$
4431	108	$E$	4500	89.0	$E$
4431	108	$E$	4500	89.0	$E$
4437	2.2	$A_1$	4504	2.0	$A_1$
4526	8.2	$E$	4573	5.2	$E$
4526	8.2	$E$	4573	5.2	$E$
4527	10.8	$A_1$	4575	5.5	$A_1$

$C3v$  symmetry with HF and [ $B3(\text{H})$ ], respectively. These frequencies are correctly found below the equivalent harmonic frequency predicted for the isolated ion [ $3538$  ( $3500$ )  $\text{cm}^{-1}$ ]. Likewise, the  $\text{H}_3^+$  degenerate bending frequency ( $2859$   $\text{cm}^{-1}$ ) is reduced by 174 and 195  $\text{cm}^{-1}$  in the  $C_s$  structure, and by 177  $\text{cm}^{-1}$  in the  $C3v$  structure. This bending frequency ( $2799$   $\text{cm}^{-1}$ ) is found reduced by 322 and 334  $\text{cm}^{-1}$  and 318  $\text{cm}^{-1}$  for  $C_s$  and  $C3v$  structures with  $B3(\text{H})$  calculations. The fact that  $B3(\text{H})$  results

gave the lowest frequencies between our two calculations could be expected since the  $H_3^+$  nucleus is relaxed with  $B3(H)$ .

Concerning the outer  $H_2$  molecules added in the  $H_{15}^+$ , we can also estimate the fundamental frequencies by the scaling procedure reported in Ref. 13 leading to 4139 and 4140  $cm^{-1}$  for the  $C_s$  structure and the  $C3v$  one, respectively. Concerning the  $B3(H)$  results, the scaling factor mentioned above has been used leading to 4118  $cm^{-1}$  for the two structures. These predictions can be connected to the weak shoulders observed near 4080–4100  $cm^{-1}$  in clusters larger than  $H_9^+$  which are certainly due to the absorption by these outer  $H_2$ .

As expected, the high frequencies are found higher within HF calculations than in DFT, in agreement with the smaller scaling factor of  $B3(H)$  vs HF previously discussed, however, the trend is found opposite for the low frequencies namely in the 50–300  $cm^{-1}$  range. This could be related to larger interactions between  $H_2$  subunits found in DF calculations as evidenced by the shortest  $H_2$ - $H_2$  distances within the cluster.

## VI. INFRARED INTENSITIES

In Tables V and VI are also presented in IR intensities obtained in HF and  $B3(H)$  calculations for the  $C_s$  and  $C3v$   $H_{15}^+$  minima. The fundamental  $\nu(A_1)$  and  $\nu(A')$  ( $H_2$  stretching in the  $H_9^+$  core in both the  $C_s$  and  $C3v$  structures) observed by Okumura and co-workers,<sup>20</sup> at 4048  $cm^{-1}$  for  $H_{15}^+$  are predicted with moderate intensity, namely, 78.3, 85.4 for the  $C_s$  structure and 89 (degenerate) for the  $C3v$  one within HF calculation. For the  $B3(H)$  calculation the values are 84.2, 103, and 108 (degenerate), respectively. Furthermore, concerning the highest frequencies of  $H_{15}^+$ , they are predicted to have low intensities; 4.0, 7.0, 2.5 km/mol in HF calculation and estimated 6.3, 18.2, 1.8 km/mol with  $B3(H)$  for the  $C_s$  structure, the corresponding values are 5.2 (degenerate) and 5.5 [8.2 (degenerate), 10.8] km/mol for the  $C3v$  one [ $B3(H)$  values in parenthesis]. Among the normal modes that might be assigned to H-H stretching, the modes at 2664 and 2685  $cm^{-1}$  for the  $C_s$  structure and 2682  $cm^{-1}$  doubly degenerate for the  $C3v$  one exhibit by far the greatest predicted IR intensities, 746 and 702 km/mol, and 707 km/mol (degenerate), respectively, in HF calculations. These values have been exalted in  $B3(H)$  results [931, 859, and 868 (degenerate), respectively].

## VII. CONCLUSIONS

To take into account the apparent high stability of  $H_{15}^+$ , as seen in some cluster size distributions and collisional experiments, it has been suggested that the structure of  $H_{15}^+$  should result of a symmetric addition of six  $H_2$  around an  $H_3^+$  core. We found that this structure is not a minimum. This statement reinforces the conclusion obtained by Diekmann and co-workers.<sup>8</sup> In their paper, they found no planar structure so that they could not confirm the Hiraoka's as-

sumption supposition concerning the relative stability of  $H_{15}^+$ . Taking into account our previous results on  $H_{11}^+$  and  $H_{13}^+$ , two minima of the potential energy hypersurface of  $H_{15}^+$  are obtained from structures corresponding to nucleation of three  $H_2$  around a  $H_9^+$  core weakly deformed. The  $C_s$  structure with two  $H_2$  subunits on one side of the  $H_3^+$ , and another one on the opposite is predicted to have the lowest total energy. We notice that this structure includes a pair of  $H_2$  molecules. The distance between the  $H_2$  molecules in this pair, e.g., 349 pm at the CISD level of theory [341 pm with  $B3(H)$ ], is not far from the value (344 pm) of the intramolecular distance in the solid hydrogen.<sup>14</sup>

This work underlines the flatness of the potential energy surface since the  $C3v$  structure lies only 0.03 eV higher in energy. One can expect a relatively large fluxionality of the structures, and a great ability to dissociate, in agreement with the low temperature used in experiments and with the Car-Parrinello dynamics performed by Stich *et al.*<sup>9,10</sup>

Indeed the stability of the  $C_s$  structure could even be questioned because of the low frequency obtained at HF level (8  $cm^{-1}$ ) which is close to the numerical accuracy limit of this kind of computation. However, this frequency is found larger within the DFT  $B3(H)$  calculations (25  $cm^{-1}$ ). As in previous work<sup>11</sup> we can underline that the  $B3(H)$  functional has permitted to obtain structures and energies of  $H_{15}^+$  cluster with a reasonable computational effort and that the structures obtained are qualitatively very similar to HF ones. Moreover, the  $C_s$  structure calculated within the CISD method is very close to HF and  $B3(H)$  ones, as well as the energetics associated to its dissociation, showing that for such a type of clusters containing rather separated subunits, the lack of size consistency of the CISD method is less dramatic than one could expect.

As already seen for  $H_{11}^+$  and  $H_{13}^+$  species, all the theoretical methods used to study these clusters underestimate the energy dissociation whereas the trends in the description of stability groups is well described. On the other hand, it is worthwhile noting that the HF approach, which totally fails to predict good structures for smallest clusters,<sup>11</sup> leads to results closer to correlated methods as far as the system grows. The  $H_{15}^+$  system is the first one where two  $H_2$  molecules in the shell surrounding the  $H_9^+$  nucleus are located at a distance similar to liquid hydrogen or hydrogen ice. The stability of the  $H_{2n+3}^+$  clusters series can be thought as a result of the interaction of a given number of hydrogen molecules with a seed consisting in a  $H_9^+$  nucleus which itself consists in a  $H_3^+$  nucleus surrounded by three  $H_2$  molecules. The mobility of the second-shell, namely, the molecules around  $H_9^+$  may be rather large since the PES of the  $H_3^+(H_{2n})$  clusters with  $n > 3$  is flat.

By inspection of the charge distribution, the Mulliken population analysis is highly significant in this kind of system because all atoms hold the same orbital basis set. The analysis obtained from the present calculations have shown that most of the +1 charge is beared by the  $H_3^+$  core (+0.60) and the  $H_2$  of the first shell ( $H_9^+$ ) (0.11 each), whereas each external  $H_2$  molecules have lost only 0.02 electrons. This is in agreement with the vibrational frequencies spectra of these clusters, for which the most external  $H_2$  molecules exhibit vibrational frequencies close to those of neutral hydrogen.

- <sup>1</sup>E. E. Ferguson, F. C. Fehsenfeld, and D. L. Albritton, in *Gas Phase Ion Chemistry*, edited by M. T. Bowers (Academic Press, New York, 1979), Vol. 1.
- <sup>2</sup>R. Clappitt and L. Gowland, *Nature (London)* **223**, 815 (1968).
- <sup>3</sup>A. Van Lumig and J. Reuss, *Int. J. Mass Spectrom. Ion Phys.* **27**, 1197 (1978).
- <sup>4</sup>K. Hiraoka and P. Kebarle, *J. Chem. Phys.* **62**, 2267 (1978); K. Hiraoka *ibid.* **87**, 4048 (1987); K. Hiraoka and T. Mori, *Chem. Phys. Lett.* **157**, 467 (1989).
- <sup>5</sup>Y. K. Bae and P. C. Cosby, *Chem. Phys. Lett.* **159**, 215 (1989).
- <sup>6</sup>W. Kohn and L. J. Sham, *Phys. Rev. A* **140**, 1133 (1965).
- <sup>7</sup>R. Car and M. Parrinello, *Phys. Rev. Lett.* **55**, 2471 (1985).
- <sup>8</sup>B. Diekmann, P. Borrmann, and E. R. Hilf, *Surf. Rev. Lett.* **3**, 253 (1996).
- <sup>9</sup>I. Štich, D. Marx, M. Parrinello, and K. Terakura, *Phys. Rev. Lett.* **78**, 3669 (1997).
- <sup>10</sup>I. Štich, D. Marx, M. Parrinello, and K. Terakura, *J. Chem. Phys.* **107**, 9482 (1997).
- <sup>11</sup>H. Chermette, H. Razafinjanahary, and L. Carrion, *J. Chem. Phys.* **107**, 10 643 (1997).
- <sup>12</sup>M. Farizon, B. Farizon-Mazuy, N. V. de Castro Faria, and H. Chermette, *Chem. Phys. Lett.* **177**, 451 (1991).
- <sup>13</sup>M. Farizon, H. Chermette, and B. Farizon-Mazuy, *J. Chem. Phys.* **96**, 1325 (1992).
- <sup>14</sup>D. Scharf, M. L. Klein, and G. J. Martyna, *J. Chem. Phys.* **97**, 3590 (1992).
- <sup>15</sup>J. P. Perdew, in *Electronic Structure of Solids '91*, edited by P. Ziesche and H. Eschrig (Academic Verlag, Berlin, 1991).
- <sup>16</sup>M. J. Frisch, G. W. Trucks, H. B. Schlegel, P. M. W. Gill, M. A. Robb, J. R. Cheeseman, T. A. Keith, G. A. Petersson, J. A. Montgomery, K. Raghavachari, M. A. Al-Laham, V. G. Zakrzewski, J. V. Ortiz, J. B. Foresman, J. Cioslowski, B. B. Stefanov, A. Nanayakkara, M. Challacombe, C. Y. Peng, P. Y. Ayala, W. Chen, M. W. Wong, J. L. Andres, G. Johnson, E. S. Replogle, R. Gomperts, R. L. Martin, D. J. Fox, J. S. Binkley, D. J. Defrees, J. Baker, J. P. Stewart, M. Head-Gordon, C. Gonzalez, and J. A. Pople, *GAUSSIAN 94 (Revision C.3)* (Gaussian, Inc., Pittsburgh, 1995).
- <sup>17</sup>S. Louc, Ph.D. thesis, Université Claude Bernard, Lyon, 1997.
- <sup>18</sup>J. P. Perdew and K. Burke, *Int. J. Quantum Chem.* **57**, 309 (1996).
- <sup>19</sup>D. C. Patton and M. R. Pederson, *Phys. Rev. A* **56**, R2495 (1997).
- <sup>20</sup>M. Okumura, L. I. Yeh, and Y. T. Lee, *J. Chem. Phys.* **83**, 3705 (1985); **88**, 79 (1988).